

Photocurrent Improvement by Incorporation of Single-Wall Carbon Nanotubes in TiO₂ Film of Dye-Sensitized Solar Cells

Kyung-hwa Jung, Song-Rim Jang, R. Vittal,[†] Donghwan Kim,[‡] and Kang-Jin Kim*

Division of Chemistry and Molecular Engineering, and CRM-COSEF, Korea University, Seoul 136-701, Korea

[†]Central Electrochemical Research Institute, Karaikudi 630 006, India

[‡]Division of Materials Sciences, College of Engineering, Korea University, Seoul 136-701, Korea

Received August 20, 2003

Single-wall carbon nanotubes (SWCN) were integrated in TiO₂ film and the beneficial influence on the dye-sensitized solar cells in terms of improved photocurrent was studied in the light of static *J-V* characteristics obtained both under illumination and in the dark, photocurrent transients, IPCE spectra and impedance spectra. Compared with a solar cell without SWCN, it is established that the photocurrent density of the modified cell increases at all applied potentials. The enhanced photocurrent density is correlated with the augmented concentration of electrons in the conduction band of TiO₂ and with increased electrical conductivity. Explanations are additionally corroborated with the help of SEM, Raman spectra and dye-desorption measurements.

Key Words : Single-wall carbon nanotubes, Photocurrent, Dye-sensitized solar cells

Introduction

There have been reports earlier that incorporation of single-wall carbon nanotubes (SWCN) in films of poly(3-octylthiophene)^{1,2} or poly(methyl methacrylate)³ enhanced electrical conductivity of the composite films. SWCN also conferred electrical conductivity to metal-oxide nanocomposites.⁴ A composite of poly(p-phenylene vinylene) with SWCN in a photovoltaic device showed good quantum efficiency, owing to the formation of a complex interpenetrating network with the polymer chains.⁵ However, no reports have been found in the literature where SWCN were used in TiO₂ films of dye-sensitized solar cells (DSC), despite their expected potential to enhance solar energy conversion efficiency due to favorable electrical conductivity. We reported earlier that incorporation of SWCN in TiO₂ film improves the short-circuit photocurrent of DSC.⁶

One of the key issues for improving conversion efficiencies of DSC is to block the surface states lying below the conduction band edge.⁷⁻⁹ Treatment with 4-*tert*-butylpyridine on the TiO₂ surface increases the photocurrent due to the reduction of an interfacial back electron transfer mediated by Ti³⁺ surface states.¹⁰ Addition of larger TiO₂ particles¹¹⁻¹⁴ or titanium silicalite-2¹⁵ to nanocrystalline TiO₂ colloidal solution increases the light scattering and the absorption in the red portion, thereby increasing the photocurrent. Recently, efforts have been made to improve the conversion efficiency through photocurrent enhancement by modification of TiO₂ film, using a TiO₂-WO₃ buffer layer,¹⁶ polypyrrole in TiO₂ film,¹⁷ and imidazolium ions instead of Li⁺ ions.¹⁸

In this paper, enhancement of photocurrent of DSC caused by incorporation of SWCN in TiO₂ is investigated by electron

microscopy, electrochemical impedance spectroscopy, and transient photocurrent measurements, in order to reinforce our earlier research on the photocurrent-voltage characteristics of the dye-sensitized solar cells.⁶

Experimental Section

Single-wall carbon nanotubes (SWCN, Carbon Nanotechnologies Inc.) were used without purification. The purity of the SWCN was evident by the enhancement of G-line at 1581 cm⁻¹ relative to D-line at 1350 cm⁻¹, using a Jasco NR 1100 Raman spectrophotometer.¹⁹ Typical diameter of the long tubes was estimated to be about 10 nm by using a Hitachi S-4300 FE-SEM. A small amount of SWCN, dispersed in N,N-dimethylformamide was mixed with P25 (Degussa) aqueous colloidal solution for preparing TiO₂ electrodes.¹⁷ SWCN can be dispersed in other solvents such as toluene, chloroform and N-methylpyrrolidone, which yield however water-immiscible solutions. Transparent TiO₂ films were obtained by spin coating the colloidal mixture on F-doped SnO₂ (FTO) conducting glass (Libbey-Owen-Ford Co.), using a spin coater from Laurell Technologies Corporation, WS-200-4NPP. The resulting film was annealed at 450 °C for 30 min in air. Surface morphology and thickness of the annealed film was estimated from FE-SEM images. Thickness was about 4 μm. X-ray diffraction (XRD) measurements were carried out using a MAC Science Co. MO3XHF X-ray diffractometer with Cu Kα radiation. The TiO₂ film thus obtained was coated with [RuL₂(NCS)₂]₂·2H₂O (hereafter Ru(II), where L=2,2'-bipyridine-4,4'-dicarboxylic acid) in 3 mM absolute ethanol for 12 h at room temperature.

Photocurrents were measured using a Keithley Model M236 source measure unit. A 250-W tungsten-halogen lamp (Oriel) was used to illuminate an area of 3 mm in diameter of the TiO₂ working electrode in acetonitrile containing 60

*Corresponding author. E-mail: kjkim@korea.ac.kr

mM LiI and 3 mM I₂. Pt gauze was used as the counter electrode. Transient photocurrent was obtained with a homemade shutter attachment. An HP 8453A diode array spectrophotometer was used for estimating dye concentration. Incident photon-to-current conversion efficiency was measured with an Aminco-Bowman FA-256 luminescence spectrometer. Electrochemical impedance spectra were recorded over a frequency range of 10⁻² to 10⁴ Hz with an ac amplitude of 5 mV using an EG&G PARC M273A potentiostat with an M1025 frequency-response detector. The data were analyzed by using ZView software (Scribner Associates, Inc.).

Results and Discussion

Figure 1 shows the cross-sectional view of an FE-SEM image of TiO₂ film incorporated with SWCN and annealed at 450 °C for 30 min in air (hereafter denoted by SWCN/TiO₂). It can be seen that TiO₂ particles and SWCN adhere to each other and that the interconnectivity of the TiO₂ particles is not affected. This observation is consistent with a recent report that SWCN act as preferential sites for the crystallization of sol-gel TiO₂.²⁰ Raman spectra (Figure 2) in

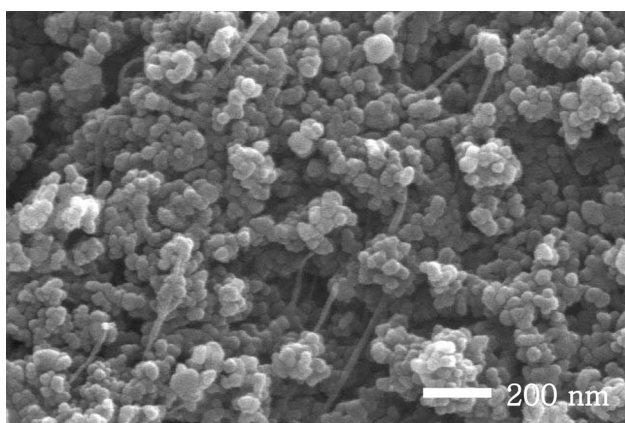


Figure 1. A cross-sectional FE-SEM view of an annealed TiO₂ film containing SWCN.

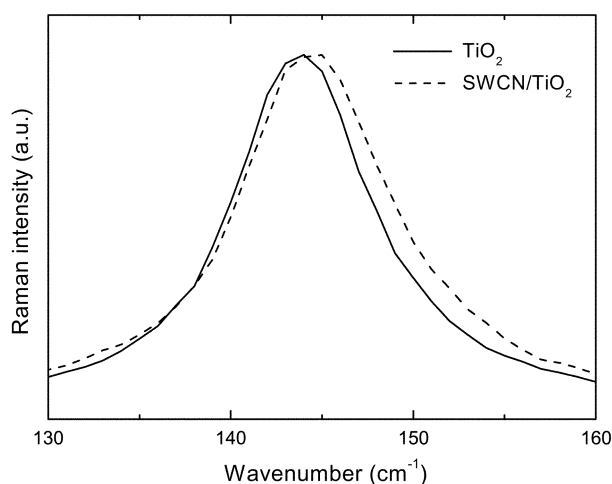


Figure 2. Raman spectra of TiO₂ and SWCN/TiO₂ films. $f = 5.5 \times 10^{-4}$.

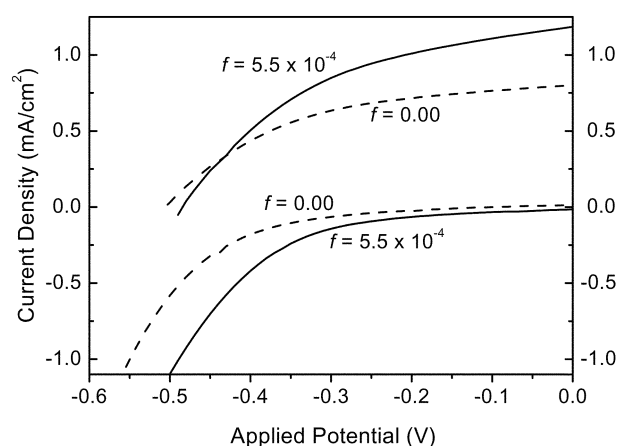


Figure 3. J - V curves of dye-sensitized solar cells prepared with SWCN/TiO₂ films. Upper two curves are under illumination and lower two in the dark.

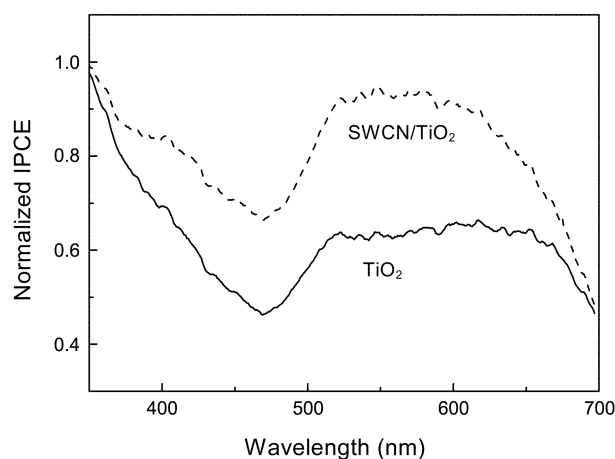


Figure 4. Normalized IPCE spectra of the solar cells prepared with TiO₂ and SWCN/TiO₂ electrodes.

the region between 120 and 160 cm⁻¹ show that the band corresponding to E_g mode of TiO₂ at 143 cm⁻¹ in case of SWCN/TiO₂ film shifts slightly to the blue by about 1.1 cm⁻¹, with an 8% increase in FWHM compared to that of the TiO₂ film, although the changes are not remarkable due to the small SWCN weight fraction f of 5.5×10^{-4} in the film. This spectral change is obviously due to the adherence of TiO₂ particles to SWCN. Up to $f = 5.5 \times 10^{-4}$, Raman spectra gave no peaks originated from SWCN, but only those of anatase phase of TiO₂.²¹ Analysis of XRD data suggests that the crystalline phase of TiO₂ remained the same with the addition of SWCN.

As reported previously, the photocurrent density increases over the applied potential range from 0 to the open circuit voltage with the SWCN incorporation in TiO₂ film.⁶ Typically the short-circuit current density (J_{sc}) increases by about 50% when f is 5.5×10^{-4} (Figure 3). The photocurrent enhancement of the cell with an SWCN/TiO₂ electrode is a result of unfailingly higher incident-photon-to-current conversion efficiency (IPCE) at all wavelengths over the visible region (Figure 4). The maximum IPCE at 540 nm with an SWCN/TiO₂ electrode at $f = 5.5 \times 10^{-4}$ is 47% higher than

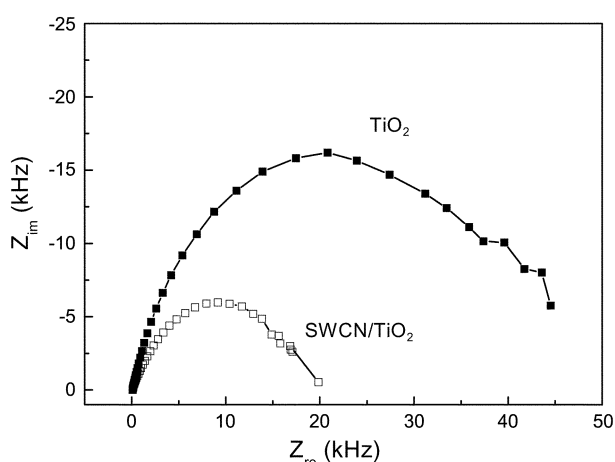


Figure 5. Nyquist plots of dye-sensitized TiO₂ and SWCN/TiO₂ cells at $f = 5.5 \times 10^{-4}$ from 10 kHz to 10 mHz. DC potential was 0.0 V and AC amplitude 5.0 mV.

that with a TiO₂ electrode, which is in good agreement with the J_{sc} increase. As the cells were not optimized for the best possible photocurrent response in terms of film thickness, type of lamp and composition of electrolyte, the photocurrent yields were generally less in our experiments, especially due to the thin TiO₂ films. A very thin layer of about 4 μm of TiO₂ was used compared with about 10 μm in usual DSC, in order to avoid needless dark films in the presence of SWCN.

One explanation for the photocurrent behavior lies in the increased electrical conductivity of the film as reported earlier.⁶ Supporting evidence for the increase in electrical conductivity is obtained with the help of electrochemical impedance spectroscopy (EIS). Figure 5 compares Nyquist plots of dye-coated TiO₂ solar cells with and without SWCN. The total impedance of the cell with SWCN is obviously smaller than that of the cell without SWCN. Each cell may be visualized as consisting of a multilayer structure to which an RC circuit in series can be fitted, so that its impedances can be modeled by an equivalent circuit.^{22,23} Analysis of EIS data, optimized by fitting to an equivalent circuit, using ZView software shows that resistance of

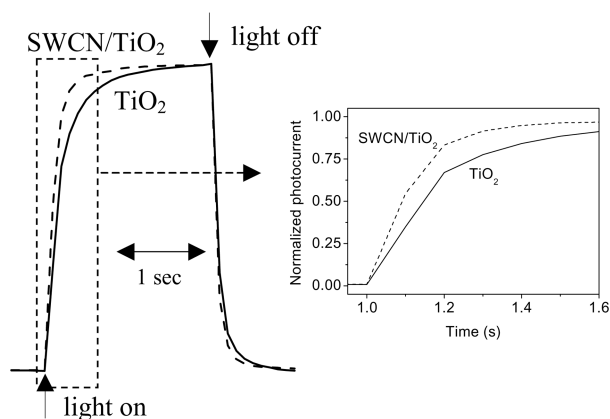


Figure 6. Normalized transient photocurrent responses of the cells prepared with TiO₂ (solid line) and SWCN/TiO₂ (dotted line) electrodes at $f = 5.5 \times 10^{-4}$.

SWCN/TiO₂ film decreases conspicuously by a factor of three compared with that of the TiO₂ film, with other resistances being essentially comparable for the two electrodes. The result is consistent with a recent result that the doping of an insulating polymer with SWCN increased electrical conductivity by several orders.^{1,2}

Further evidence for the photocurrent enhancement is obtained from transient photocurrent responses of the cells, which are recorded at several on-off cycles of illumination. A representative trace is shown in Figure 6, which is normalized at the maximum photocurrent density. When the light is switched on and off, photocurrent response of an SWCN/TiO₂ electrode rises and falls faster than that of a TiO₂ electrode, even though the difference appears to be minute, again due to the small concentration of SWCN, at $f = 5.5 \times 10^{-4}$, in the film. For example, the time required for the photocurrent density to rise from zero to 90% of the total change of an SWCN/TiO₂ electrode is about 0.3 s faster than that of a TiO₂ electrode. Electrons trapped in the surface states appear to be responsible for the slow photocurrent response.^{24,25} Figure 6 thus suggests that SWCN/TiO₂ facilitates a decrease of trapping surface states due to their blocking by SWCN, which is consistent with the photocurrent enhancement in this case.

However, the amount of dye, desorbed from the surface of SWCN/TiO₂ film, was found to be smaller than that from the film without SWCN, showing that Ru(II) dye molecules do not adsorb to SWCN. This can be explained by the FE-SEM data in Figure 1 SWCN are not only poorly attached to TiO₂ particles, but also non-uniformly distributed in the film, which can reduce the amount of adsorbed dye in the TiO₂ film layer. The poor adsorption of dye in SWCN/TiO₂ film results in an offset of the photocurrent increase with SWCN.

Under the dark condition, current density of the cell with an SWCN/TiO₂ electrode is larger than that without SWCN at all applied potentials (Figure 3). This result implies that back electron transfer given in eq. 1 is facilitated with the SWCN incorporation in the TiO₂ film,



where e_{cb}^- represents electrons in the conduction band of TiO₂. The cause of the dark current density increase with the incorporation can be related to the increase in the triiodide ion I_3^- concentration, since e_{cb}^- is not expected to increase with the incorporation of SWCN. Probably, poorly attached SWCN in the SWCN/TiO₂ film electrode creates more void volume compared with a TiO₂ film electrode, causing the triiodide ion concentration to increase in the SWCN/TiO₂ film. Increase in triiodide ion concentration leads to an enhancement of the back electron transfer, resulting in the dark current increase. The increase in the dark current density is consistent with the decrease in open-circuit voltage (V_{oc}) with the SWCN incorporation, which is observed in Figure 3. The V_{oc} decrease indicates that the conduction band edge of TiO₂ is lowered, facilitating the back electron transfer.²⁶

Finally, one may argue that SWCN can also inject electrons into the conduction band of TiO₂. It is however

observed that photocurrent is not generated by SWCN/TiO₂ electrode in the absence of dye, indicating that SWCN do not act as sensitizers.

Conclusion

Enhancement of the photocurrent of dye-sensitized solar cells (DSC) caused by incorporation of single-wall carbon nanotubes (SWCN) in TiO₂ film electrodes was studied. Compared with an unmodified cell, the modified cell shows an increase in short-circuit photocurrent as much as 50%, when the SWCN weight fraction in TiO₂ film is 5.5×10^{-4} . The photocurrent increase is a result of unfailingly higher incident-photon-to-current conversion efficiency at all wavelengths over the visible region. The enhanced photocurrent is correlated with an augmented concentration of free conduction band electrons and increased electrical conductivity in the presence of SWCN in the TiO₂ film electrode. A decrease in trapping surface states is inferred in case of film incorporated with SWCN, with the help of transient photocurrent measurements. The increased electrical conductivity is evidenced by electrochemical impedance spectra. It is emphasized that SWCN incorporation in TiO₂ film provides better electron transfer through the film in the DSC.

Acknowledgement. The Korea Research Foundation Grant (2001-015-DP0371) financially supported this work.

References

1. Kymakis, E.; Alexandou, I.; Amaratunga, G. A. J. *Synth. Met.* **2002**, *127*, 59.
2. Musa, I.; Baxendale, M.; Amaratunga, G. A. J.; Eccleston, W. *Synth. Met.* **1999**, *102*, 1250.
3. Hagenmueller, R.; Gommans, H. H.; Rinzler, A. G.; Fischer, J. E.; Winey, K. I. *Chem. Phys. Lett.* **2000**, *330*, 219.
4. Flahaut, E.; Peigney, A.; Laurent, Ch.; Marlière, Ch.; Chastel, F.; Rousset, A. *Acta Mater.* **2000**, *48*, 3803.
5. Ago, H.; Petrisch, K.; Shaffer, M. S. P.; Windle, A. H.; Friend, R. H. *Adv. Mater.* **1999**, *11*, 1281.
6. Jung, K.-H.; Hong, J. S.; Vittal, R.; Kim, K.-J. *Chem. Lett.* **2002**, *31*, 864.
7. Huang, S. Y.; Schlichthörl, G.; Nozik, A. J.; Grätzel, M.; Frank, A. J. *J. Phys. Chem. B* **1997**, *101*, 2576.
8. Schlichthörl, G.; Huang, S. Y.; Sprague, J.; Frank, A. J. *J. Phys. Chem. B* **1997**, *101*, 8141.
9. Moser, J.; Punchedhewa, S.; Infelta, P. P.; Grätzel, M. *Langmuir* **1991**, *7*, 3012.
10. Nazeeruddin, M. K.; Kay, A.; Rodicio, I.; Humphry-Baker, R.; Müller, E.; Liska, P.; Vlachopoulos, N.; Grätzel, M. *J. Am. Chem. Soc.* **1993**, *115*, 6382.
11. Barbé, C. J.; Arendse, F.; Comte, P.; Jirousek, M.; Lenzenmann, F.; Shklover, V.; Grätzel, M. *J. Am. Ceram. Soc.* **1997**, *80*, 3157.
12. Ferber, J.; Luther, J. *Sol. Energy Mater. Sol. Cells* **1998**, *54*, 265.
13. Rothenberger, G.; Comte, P.; Grätzel, M. *Sol. Energy Mater. Sol. Cells* **1999**, *58*, 321.
14. Usami, A. *Sol. Energy Mater. Sol. Cells* **1999**, *59*, 163.
15. Kang, M. G.; Park, N.-G.; Chang, S. H.; Choi, S. H.; Kim, K.-J. *Bull. Korean Chem. Soc.* **2002**, *23*, 140.
16. Kang, T.-S.; Moon, S.-H.; Kim, K.-J. *J. Electrochem. Soc.* **2002**, *149*, E155.
17. Hong, J. S.; Joo, M.; Vittal, R.; Kim, K.-J. *J. Electrochem. Soc.* **2002**, *149*, E493.
18. Park, N.-G.; Chang, S. H.; van de Lagemaat, J.; Kim, K.-J.; Frank, A. J. *Bull. Korean Chem. Soc.* **2000**, *21*, 985.
19. Holden, J. M.; Zhou, P.; Bi, X.X.; Eklund, P. C.; Bandow, S.; Jishi, R. A.; Chowdhury, K. D.; Dresselhaus, G.; Dresselhaus, M. S. *Chem. Phys. Lett.* **1994**, *220*, 186.
20. Vincent, P.; Brioude, A.; Jourmet, C.; Rabaste, S.; Purcell, S. T.; Le Brusq, J.; Plenet, J. C. *J. Non-Cryst. Solids* **2002**, *311*, 130.
21. Park, N.-G.; Schlichthörl, G.; van de Lagemaat, J.; Cheong, H. M.; Mascarenhas, A.; Frank, A. J. *J. Phys. Chem. B* **1999**, *103*, 3308.
22. Hauch, A.; Kern, R.; Feeber, J.; George, A.; Luther, J. *2nd World Conference and Exhibition on Photovoltaic Solar Energy Conversion*; Vienna, 1998; p 260.
23. Kang, T. S.; Chun, K. H.; Hong, J. S.; Moon, S. H.; Kim, K. J. *J. Electrochem. Soc.* **2000**, *147*, 3049.
24. Schwartzburg, K.; Willig, F. *Appl. Phys. Lett.* **1991**, *58*, 2520.
25. Qian, X.; Qin, D.; Song, Q.; Bai, Y.; Li, T.; Tang, X.; Wang, E.; Dong, S. *Thin Solid Films* **2001**, *385*, 152.
26. Diamant, Y.; Chen, S. G.; Melamed, O.; Zaban, A. *J. Phys. Chem. B* **2003**, *107*, 1977.